Investigation of the fluctuation properties of the ion saturation current in the edge and divertor plasmas in LHD

S. Masuzaki, N. Ohno [a], V.P. Budaev [b], S. Sakakibara, T. Morisaki, M. Kobayashi, N. Ohyabu, A. Komori and the LHD Experimental Group

National Institute for Fusion Science,322-6 Oroshi-cho, Toki 509-5292, Japan
[a] Eco Topia Science Institute, Nagoya University, Nagoya 464-8603, Japan
[b] Nuclear Fusion Institute, RRC Kurchatov Institute, 123182, Kurchatov Sq.1, Moscow, Russia

(Received day month year / Accepted day month year should be centered 10-point type)

Fluctuation properties of the ion saturation current measured by using Langmuir probes in the edge and divertor plasmas were investigated based on probability distribution function (PDF) analysis in the Large Helical Device (LHD). In the edge plasma region, both positive and negatively skewed PDFs were observed. Unlike tokamak cases, negatively skewed PDFs were found at divertor legs. On a divertor plate, sign of skewness of I_{sat} PDF inverts from positive to negative value during a discharge.

Keywords: Large Helical Device (LHD), edge plasma, divertor plasma, ion saturation current, fluctuation, intermittent events, probability distribution function (PDF)

1. Introduction

In magnetic fusion devices, energy and particle fluxes crossing the last closed flux surface (LCFS) are transported to plasma facing components conductively and convectively in scrape-off layer (SOL). The distributions of heat and particle loads on plasma facing components are very important parameters for designing devices, and are determined by the balance between the parallel and perpendicular transports. The perpendicular transport coefficients, such as diffusion coefficient are anomalous, and fluctuation phenomena are believed to strongly relate to the transport [1].

In tokamaks, it is widely observed that SOL consists of the near- and far-SOL [2]. The difference between these regions is the density decay length. In the near-SOL, just outside LCFS, the density profiles are usually exponential with short (a few cm) decay length. On the other hand, the decay length is long, and the profiles are nearly flat in the far-SOL. Therefore plasma with substantial density exists in front of main chamber first wall, and the particle load on first wall cannot be ignored. The transport in the far-SOL is believed to be not diffusive but convective associated with intermittent events, so called ‘blob’, and the probability distribution function (PDF) of the density fluctuations in the far-SOL has non-Gaussian tail.

In the Large Helical Device (LHD), the world largest superconducting helical device with heliotron-type magnetic configuration, there is a unique edge magnetic field lines structure. There exist an intrinsic stochastic layer just outside of LCFS, residual islands embedded in the stochastic layer, the edge surface layers and the intrinsic divertor structure (helical divertor), this magnetic structure is one of the characteristics of the heliotron-type configuration [3]. Figure 1 (a) shows a Poincare plot of magnetic field lines in a horizontally elongated cross-section in LHD. Blue and red points outside LCFS indicate open field lines striking divertor plates. Yellow lines are contours of magnetic field strength, and they show that the gradient of magnetic field strength largely changed in a poloidal cross-section. For the difference of magnetic structure in the edge plasma region, comparison the fluctuation properties in the edge and divertor plasmas between tokamaks and helical devices could make it possible to understand the physics of cross-field transport.

It was reported that the intermittent properties of I_{sat} measured by a Langmuir probe on a divertor plate is similar to that observed in tokamaks SOL and linear divertor simulator [4]. It was observed that large positive and negative bursty signals dominates the time-evolutions of I_{sat} measured at lower field side and striking point of the divertor leg, respectively, and this is consistent with theoretical prediction of blob transport [5]. In this paper, the fluctuation properties of the ion saturation current, I_{sat}, measured by Langmuir probes in the edge and divertor

author’s e-mail: masuzaki@LHD.nifs.ac.jp

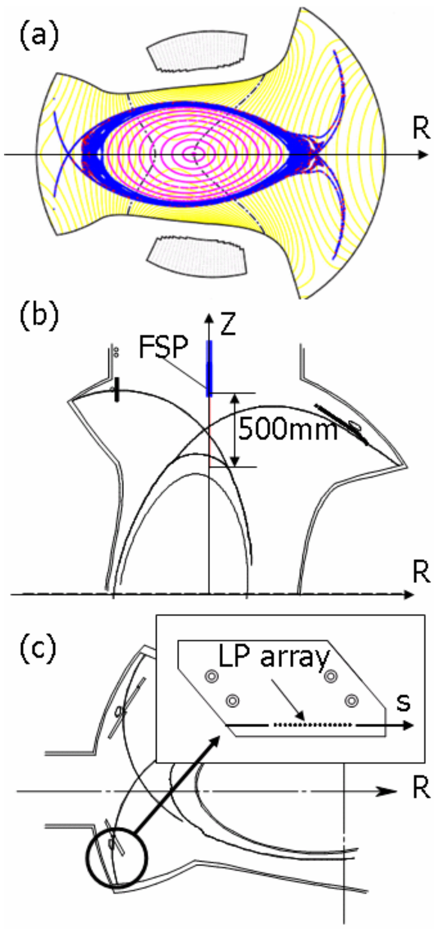

Fig. 1 (a) Poincare plot of magnetic field lines in a horizontally elongated cross-section in LHD. Blue and red points outside LCFS indicates open field lines striking divertor plates. Yellow lines are contours of magnetic field strength. Poloidal cross-sections of LHD plasma and vacuum vessel at the positions of (b) FSP (fast scanning Langmuir probe) and of (c) the divertor plate in which LP array is installed, respectively.

plasmas in the unique edge magnetic structure are investigated based on PDF analysis.

2. Experimental set-up

Hydrogen plasmas heated and sustained by neutral beam injection (NBI) are investigated in this study. Figure 1 (b) and (c) show positions of the Langmuir probes. Fast scanning Langmuir probe (FSP) moves 500 mm vertically from the top wall along Z-axis as shown in Fig. 1(b) using a pneumatic cylinder. The position of first wall is Z~1.6 m. The maximum velocity of FSP is about 1 m/s. One electrode made of graphite, dome-type with 2 mm of diameter, was provided for this study, and I_{sat} profiles along Z-axis were measured. On the divertor plate which locates torus inboard-side in the horizontally elongated cross-section, there is a Langmuir probe array (LP array) consisting of 16 dome-type electrodes with a 2 mm of diameter as shown in Fig. 1(c). The distance between electrodes is 6 mm, and I_{sat} profiles along S-axis were obtained. S-axis is along the edge of the divertor plate, and the direction is almost toroidal. Sampling frequencies and dynamic ranges of the LP array and FSP for their data acquisition are 500 kHz and 1 MHz, respectively.

3. Results and discussions

The fluctuation properties of I_{sat} signals measured by Langmuir probes were analyzed based on PDF analysis. For fully random signal, PDF has a Gaussian distribution. The deviation of PDF from Gaussian distribution function can be characterized by skewness, $S = \langle x^3\rangle/\langle x^2\rangle^{3/2}$, and flatness, $F = \langle x^4\rangle/\langle x^2\rangle^2$. Skewness and flatness are measures of asymmetry and of the tail's weight with respect to core of PDF, respectively, and $S = 0$, $F = 3$ for Gaussian distribution.

3.1 Result of the edge plasma measurement

I_{sat} profiles in the edge plasma were measured by FSP during discharges with a magnetic configuration of R_{ax} = 3.60 m, where R_{ax} is major radius of magnetic axis. Figures 2(a) and (b) show an I_{sat} profile during a discharge with 2×10^{19} m^{-3} of line averaged electron density and 3 MW of NBI heating power and field lines connection length, L_c, profile along Z-axis calculated with field lines tracing code, respectively. Smaller Z is closer to LCFS. Field lines trace

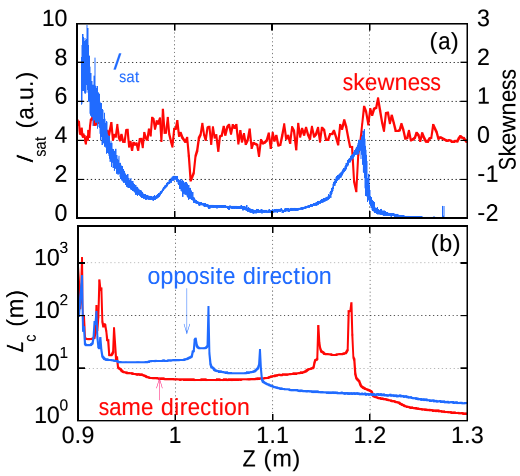

Fig. 2 (a) I_{sat} profile along Z axis measured by using FSP and skewness profile estimated using every 1000 data points. (b) Profiles of connection length of magnetic field lines (L_c) along Z axis calculated with field lines tracing code. Red and blue lines show L_c profiles calculated for same and opposite directions of magnetic field direction, respectively.

was conducted for two directions. One is the same direction as magnetic field, and another one is the opposite direction. Two I_{sat} peaks appear at Z = 1.0 m and 1.2 m, and they correspond to long L_c groups positions in Fig. 2 (b). The difference of positions between I_{sat} peaks and L_c peaks is considered to be caused by the alignment error of FSP. These long field lines approach the vicinity of LCFS, and they are main channel of particle and energy flow from LCFS to divertor. On the other hand, field lines less than 100 m do not approach LCFS [6].

Skewness profile is also plotted in Fig. 2(a). Skewness was estimated after removing DC component from raw I_{sat} signal using high-pass digital filter (>100Hz), and using 1000 data points (1 ms). Therefore the spatial resolution of this analysis is about 1 mm. In tokamaks, negative skewness has been observed near or inside LCFS, and skewness is positive and becomes larger with increase the distance from LCFS [7]. In LHD R_{ax}=3.60 m configuration case, there are two negative peaks at the vicinity of I_{sat} peaks (Z ~ 1.02 m and ~ 1.18 m) , that is the vicinity of L_c peaks as shown in Fig. 2. This result indicates that negative bursts corresponding to density drops are dominant in this region. Fig. 2(b) shows that these field lines at the L_c peak positions connect to divertor plates less than 10 m, and that means these peaks are divertor legs. Relatively large positive skewness appears beside negative peaks of skewness as shown in Fig. 2(a). This observation is consistent with previous observation in divertor plasma [5]. From Z ~ 1.20 m to 1.28 m, skewness decreases from 1 to 0 with decay length of 2 cm, and I_{sat} becomes noise level at Z > 1.28 m. It suggests that transport becomes diffusive in the outermost region. Assuming the positive spikes in I_{sat} at Z > 1.21 m region are blobs, a possible explanation of determining the decay length of skewness is lifetime of blobs. Lifetime of blob is roughly estimated as L_c/C_s, where C_s is ion sound speed. In the case of around Z = 1.21 m, L_c ~ 10 m and C_s ~ 3×10^4 m/s (assuming T_e = 10eV), and the lifetime is ~ 0.3 ms. Assuming blob speed to be 100 - 1000 m/s, the propagation length is 3 - 30 cm.

3.2 Temporal change of PDF property in divertor plasma

Temporal change of PDF property of I_{sat} measured by Langmuir probe array on a torus-outboard divertor plate (see Fig. 1(c)) was observed during discharges with R_{ax} = 3.60 m and P_{NBI} = 5.9 MW. Typical waveforms of plasma parameters in such a discharge are shown in Figs. 3(a)-(c). Normalized I_{sat} profiles on the Langmuir probe array at t = 1.3 s and 1.8 s are depicted in Fig. 3(d). In Fig. 3(c), time-evolution of skewness and flatness of I_{sat} signal at the peak of the I_{sat} profile are depicted. Skewness increases in the early phase of neutral beam injection, and it has peak at t ~ 1.4 s. Then it decreases gradually, and it becomes

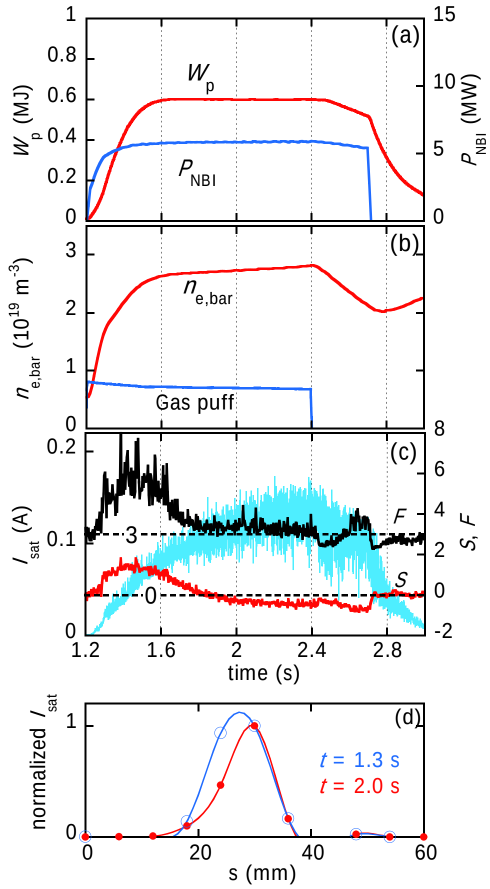

Fig. 3 Typical time evolutions of (a) stored energy, W_p, and neutral beam deposition power, P_{NBI}, (b) line averaged density, $n_{e,bar}$, and gas-puff, (c) I_{sat}, skewness (S) and flatness (F) during a discharge with magnetic configuration of R_{ax} = 3.60 m. (d) I_{sat} profile on the Langmuir probe array during same dischage. Horizontal axis is probe position (see Fig. 1(c)). Blue and red lines are fitting results.

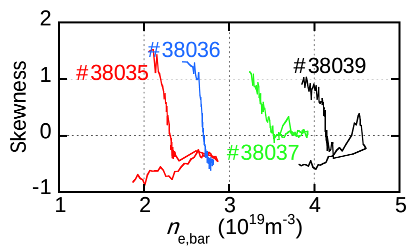

Fig. 4 Skewness of I_{sat} as a function of line averaged density.

negative after t ~ 1.8 s. The negative sign of skewness is kept until the NBI termination, and then skewness and flatness become 0 and 3, respectively. To reveal the key parameters of changing sign of skewness, electron density and temperature dependences of skewness were investigated. A series of discharges with different densities ($n_{e,bar}$ = 2 - 4×10^{19}m^{-3}) were conducted. In Fig. 4,

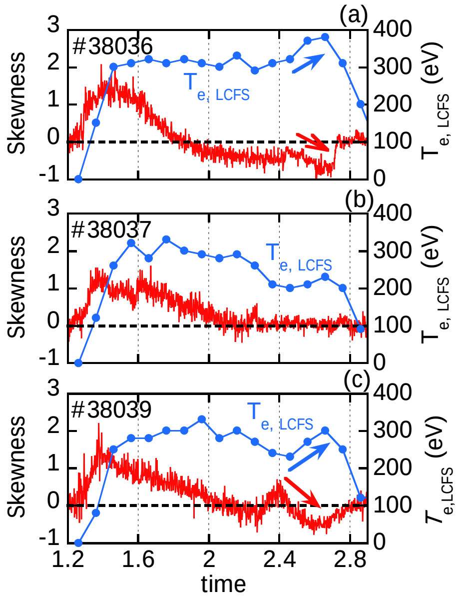

Fig. 5 Time-evolutions of skewness of I_{sat} and electron temperature at LCFS, $T_{e,LCFS}$, during the same series of discharge as Fig. 4.

skewness of I_{sat} in each discharge is plotted as a function of line averaged density, and the figure suggests that inversion of skewness sign does not depend on electron density. Figure 5 shows time-evolutions of skewness of I_{sat} and electron temperature at LCFS in the same series of discharges as Fig. 4. Skewness increases during electron temperature increase, and then decreases during electron temperature is almost constant. It seems that skewness does not depend on $T_{e,LCFS}$ in the later phase. In Fig. 5(a), sign of skewness becomes negative after t ~ 1.8 s. On the other hand, in Fig. 5(b), skewness becomes 0 at t ~ 2.1 s, and it is kept until t = 2.9 s. The difference between Figs. 5(a) and (b) is electron temperature at LCFS. In the former case, $T_{e,LCFS}$ ~ 300 eV and ~ 200eV in the latter case. This result suggests that skewness depend on $T_{e,LCFS}$, and its sign does not become negative when $T_{e.LCFS}$ is around 200 eV. In Fig. 5(c), skewness increases at t ~ 2.3 s with decrease of $T_{e.LCFS}$, and decreases from t ~ 2.4 s with increase of $T_{e.LCFS}$. This result also suggests that skewness depends on $T_{e,LCFS}$.

In Fig. 4(d), two I_{sat} profiles are shown. They are in positive (t = 1.3 s) and negative (t = 2.0 s) skewness phases, respectively. From the fitting results, the peak of I_{sat} profile shifts about 3 mm, and this shift is considered to be caused by modification of magnetic field lines structure. Modification of magnetic field lines structure could be a cause of the inversion of skewness sign. As described in section 3.1, it was observed that the negative skewness region in divertor leg is narrow, and at the vicinity of that, there is positive skewness rergion. Therefore, a small movement of magnetic structure on the divertor plate due to some reason such as a small change of rotational transform caused by toroidal plasma current could change the sign of skewness.

4. Summary

Fluctuation properties of I_{sat} in the edge and divertor plasmas in LHD were investigated based on PDF analysis.

In the LHD edge plasma region, skewness of PDF of I_{sat} has both positive and negative values, and negative region is relatively narrow. Negative peaks of skewness appear at the positions of divertor legs. In the outermost region of the edge plasma, skewness decrease from ~1 to 0 with the decay length of a few cm. This decay length is comparable to the blob propagation length roughly estimated from the lifetime of blob.

On a torus-outboard divertor plate, it was observed that the sign of skewness inverts from positive to negative at a probe channel during a discharge. Electron density does not affect this behavior but electron temperature and/or modicication of magnetic field lines structure at the divertor plate caused by toroidal plasma current could affect it.

Acknowledgements

This work was supported by the NIFS budget NIFS06ULPP511.

References

[1] B.A. Carreras, J. Nucl. Mater. **337-339**, 315 (2005).
[2] B. Lipschultz et al., Nucl. Fusion **47**, 1189 (2007).
[3] N. Ohyabu *et al*., Nucl. Fusion **34**, 387 (1994).
[4] V.P. Budaev *et al*., Plasma Fusion Res. **1**, 001 (2006).
[5] N. Ohno *et al*., Contrib. Plasma Phys. **46**, 692 (2006).
[6] S. Masuzaki *et al*, Nucl. Fusion **42**, 750 (2002).
[7] J.A. Boedo *et al*, Phys. Plasma **10**, 1670 (2003).